Journal of Hydrology, 142 (1993) 251–271
Elsevier Science Publishers B.V., Amsterdam

[1]

Critical shear stress and critical flow rates for initiation of rilling

J.E. Gilley[a], W.J. Elliot[b], J.M. Laflen[c] and J.R. Simanton[d]

[a]*USDA-ARS, University of Nebraska, Lincoln, NE 68583, USA*
[b]*Agricultural Engineering Department, Ohio State University, Columbus, OH 43210, USA*
[c]*USDA-ARS, Purdue University, W. Lafayette, IN 47907, USA*
[d]*USDA-ARS, Tucson, AZ 85719, USA*

(Received 5 May 1992; accepted 8 June 1992)

ABSTRACT

Gilley, J.E., Elliot, W.J., Laflen, J.M. and Simanton, J.R., 1993. Critical shear stress and critical flow rates for initiation of rilling. J. Hydrol., 142: 251–271.

This study was conducted to identify critical shear stress and critical flow rates required to initiate rilling on selected sites. The data used in this investigation were collected from soils located throughout the USA where crop residues had been removed, and moldboard plowing and disking had occurred. Runoff and soil loss measurements were made on sites where simulated rainfall was applied to preformed rills. Multiple regression analyses were used to relate critical shear stress values and critical flow rates to selected soil properties. The soil-based regression equations were found to provide reliable estimates. Information identified in this study will improve our ability to understand and properly model upland runoff and erosion processes.

INTRODUCTION

The force per unit wetted area that acts on a surface is defined as shear stress, τ, and is expressed as

$$\tau = \gamma y S \tag{1}$$

where γ is the specific weight of water, y is the flow depth, and S is the slope gradient. Critical shear stress, τ_c, occurs when the shear force exceeds the critical limit for soil detachment. The beginning of motion of soil particles is difficult to define. The most dependable data concerning incipient soil particle movement have resulted from laboratory experiments.

Several equations for estimating bed load sediment transport have been

Correspondence to: J.E. Gilley, USDA-ARS, University of Nebraska, Lincoln, NE 68583, USA.

0022-1694/93/$06.00

derived which use shear stress as an independent variable (Laursen, 1958). These relations were originally developed to predict sediment transport in stream and river systems. Foster (1982) used similar concepts to derive the following equation for estimating rill sediment detachment capacity, D_c:

$$D_c = K_r(\tau - \tau_c) \quad (2)$$

where K_r is the rill soil erodibility factor. This equation was used in an erosion prediction model described by Nearing et al. (1989). Equation (2) can be rearranged to yield

$$\tau = \frac{D_c}{K_r} + \tau_c \quad (3)$$

The intercept of eqn. (3) is critical shear stress, and the inverse of the slope is the rill soil erodibility factor.

Schoklitsch (1957) developed an equation which related bed load sediment transport to flow rate and slope gradient. A similar relation could be used to predict rill sediment detachment capacity where

$$D_c = K_f(QS^{3/2} - Q_cS^{3/2}) \quad (4)$$

and K_f is the flow-related rill soil erodibility factor, Q is the flow rate, and Q_c is the critical flow rate.

Equation (4) can be rearranged to yield

$$Q = \frac{1}{K_f}\left(\frac{D_c}{S^{3/2}}\right) + Q_c \quad (5)$$

Critical flow rate is represented by the intercept of eqn. (5), and the inverse of the slope is the flow-related rill soil erodibility factor.

PROCEDURE

Sediment detachment capacity was determined by Elliot et al. (1989) on soils located throughout the USA. The location, slope and particle size analyses of the soils are presented in Table 1. The soils were selected to cover a broad range of physical, chemical, mineralogical and biological properties. These properties resulted from diverse soil-forming factors acting through time, including climate, parent material, vegetation, biological activity, and topography. Each of the soils is considered to be of regional or national importance.

The study areas were located on uniform slopes having homogeneous soil characteristics. Either corn or small grains had been planted the previous year. All surface residue was first removed, and the area was then moldboard

TABLE I

Location, slope and particle size analyses of selected soils

Soil	Location		Average rill slope (%)	Particle size analysis (% by weight)		
	County	State		Sand	Silt	Clay
Academy	Fresno	CA	4.5	62.7	29.1	8.2
Amarillo	Howard	TX	3.6	85.0	7.7	7.3
Barnes-MN	Stevens	MN	8.3	48.6	34.4	17.0
Barnes-ND	Sheridan	ND	5.8	39.5	36.0	24.5
Caribou	Aroostook	ME	8.8	47.0	40.3	12.7
Cecil	Oconee	GA	4.5	64.6	15.6	19.8
Collamer	Tompkins	NY	8.7	7.0	78.0	15.0
Frederick	Washington	MD	12.8	25.1	58.3	16.6
Gaston	Rown	NC	6.4	35.5	25.4	39.1
Grenada	Panola	MS	8.7	2.0	77.8	20.2
Heiden	Falls	TX	3.9	8.6	38.3	53.1
Hersh	Valley	NE	6.6	74.4	15.9	9.7
Hiwassee	Oconee	GA	4.0	63.7	21.6	14.7
Lewisburg	Whitley	IN	7.5	38.5	32.2	29.3
Manor	Howard	MD	8.6	43.6	30.7	25.7
Mexico	Boone	MO	3.9	5.3	68.7	26.0
Miami	Montgomery	IN	5.8	4.2	72.7	23.1
Miamian	Montgomery	OH	8.9	30.6	44.1	25.3
Nansene	Whitman	WA	6.1	20.1	68.8	11.1
Opequon	Allegany	MD	12.0	37.7	31.2	31.1
Palouse	Whitman	WA	6.5	9.8	70.1	20.1
Pierre	Jackson	SD	6.6	9.6	40.9	49.5
Portneuf	Twin Falls	ID	5.6	21.5	67.4	11.1
Sharpsburg	Lancaster	NE	5.7	4.8	55.4	39.8
Sverdrup	Grant	MN	4.2	75.3	16.8	7.9
Tifton	Worth	GA	4.6	86.4	10.8	2.8
Whitney	Fresno	CA	7.4	71.0	21.8	7.2
Williams	Sheridan	ND	5.1	41.6	32.4	26.0
Woodward	Harper	OK	7.1	43.7	42.4	13.9
Zahl	Roosevelt	MT	7.6	46.3	29.7	24.0

plowed 3–12 months before the tests were conducted. After plowing, sites were disked lightly then maintained free of vegetation either by tillage or application of herbicide.

Soil samples for site characterization were obtained and analyzed using standard procedures (Soil Survey Staff, 1984). Samples were collected at a

TABLE 2

Mean, minimum and maximum values of selected soil properties at the study sites

Soil property	Mean	Minimum	Maximum
Aluminum[a]	0.15	0.03	0.50
Calcium[b]	9.0	0.0	33
Cation exchange capacity[b]	15	1.7	39
Clay[a]	21	2.8	53
Coefficient of linear extensibility[c]	0.03	0.00	0.10
Iron[a]	1.2	0.20	4.5
Magnesium[b]	2.7	0.10	9.2
Organic carbon[a]	1.2	0.16	3.3
Potassium[b]	0.65	0.10	2.5
Sand[a]	40	2.0	91
Silt[a]	39	5.5	78
Sodium[b]	0.09	0.00	0.60
Soil water content at 0.3 MPa[a]	21	4.9	34
Soil water content at 1.5 MPa[a]	9.6	1.1	19
Very fine sand[a]	12	1.1	44
Water dispersible clay[a]	8.3	1.1	25

[a] Values in %.
[b] Values in centimoles per kilogram.
[c] Values in centimeters per centimeter.

central location and at several satellite points as is typical in a standard soil survey. The following properties were measured at each site: cation exchange capacity; coefficient of linear extensibility; dithionite-citrate extractable aluminum and iron content; exchangeable calcium, magnesium, potassium and sodium; percentage of sample consisting of clay, organic carbon, sand, silt, very fine sand and water dispersible clay; and water retained by a soil sample at 0.3 and 1.5 MPa tension. Mean, minimum and maximum values of selected soil properties at the study sites are shown in Table 2.

A plot diagram of a rainfall simulation site is shown in Fig. 1. The study areas were disked immediately preceding testing. Six rills, 0.46 m across the slope by 9.0 m long, were formed using a ridging tool mounted on a small tractor. A sheet metal border was placed at the top of each rill and a runoff collection device was located at the bottom. Details and dimensions of the rill plots are presented in Fig. 2.

A portable rainfall simulator designed by Swanson (1965) was used to apply rainfall at an intensity of approximately 62 mm h^{-1}. Erosion data collection was divided into three periods: (1) rainfall only until equilibrium of rill flow occurred; (2) rainfall plus flow addition in increments at the top of

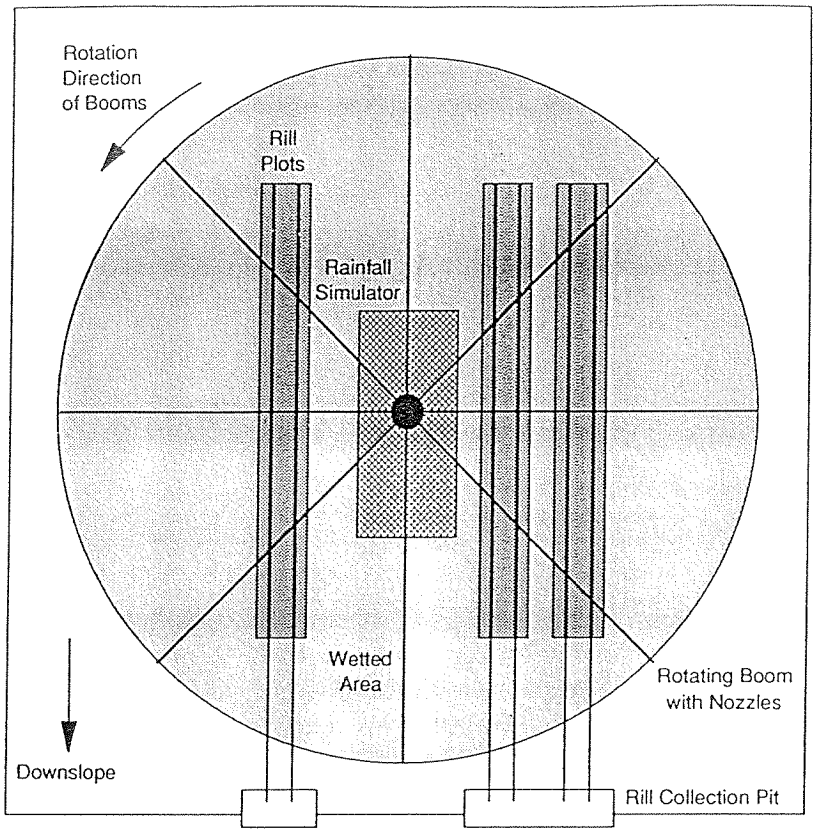

Fig. 1. Plot diagram of a rainfall simulation site.

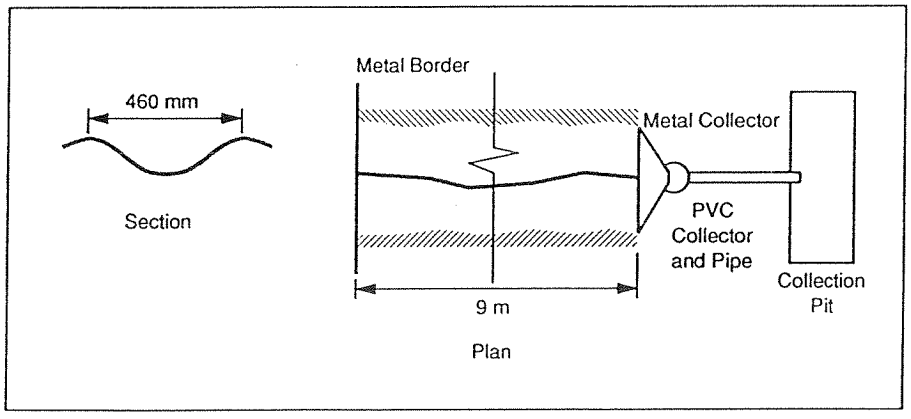

Fig. 2. Details and dimensions of the rill plots.

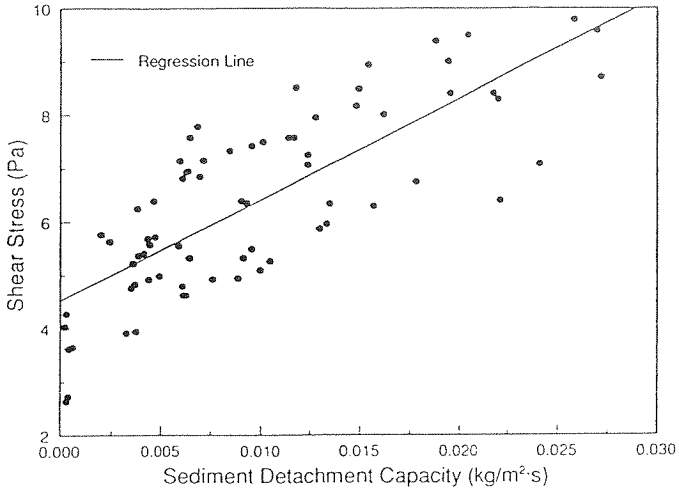

Fig. 3. Shear stress vs. sediment detachment capacity for a Barnes soil in North Dakota.

each rill; (3) flow addition at the top of each rill without rainfall. Only data obtained during the third simulation period were used in this investigation.

Flow was added to the top of each rill at rates of 7, 14, 21, 28 and 35 l min^{-1}. For each inflow rate increment, two (replicate) runoff samples were obtained from each rill under equilibrium conditions for determination of flow rate and sediment concentration. Each rill was then treated as a separate replication in the statistical analyses. Additional details concerning experimental procedures are given by Elliot et al. (1989).

CRITICAL SHEAR STRESS

Identifying critical shear stress

Shear stress vs. detachment capacity for a Barnes soil in North Dakota is shown in Fig. 3. Results obtained for this soil are also representative of the other experimental sites. It can be seen from Fig. 3 that a linear equation can be used to represent the relationship between shear stress and sediment detachment capacity. The point where the regression line intercepts the y-axis represents critical shear stress for initiation of rilling. Critical shear stress for the Barnes soil in North Dakota was 4.53 Pa.

The critical shear stress values shown in Table 3 were obtained using linear regression analyses. Positive values of critical shear stress were found for each of the experimental soils. Critical shear stress ranged from 1.73 Pa for the Sverdrup soil to 10.6 Pa for the Opequon soil.

TABLE 3

Statistical analyses of equations used to relate rill shear stress to detachment capacity

Soil	τ_c[a] (Pa)	K_r[a] ($s\,m^{-1}$) (multiply by 10^{-2})	Coefficient of determination r^2
Academy	1.82	0.704	0.833
Amarillo	1.92	4.76	0.634
Barnes-MN	5.70	1.30	0.638
Barnes-ND	4.53	0.529	0.611
Caribou	7.07	0.276	0.610
Cecil	2.56	0.455	0.624
Collamer	5.86	1.32	0.718
Frederick	9.54	0.402	0.644
Gaston	2.54	0.300	0.613
Grenada	6.39	0.725	0.606
Heiden	1.94	0.752	0.682
Hersh	3.14	1.49	0.621
Hiwassee	1.94	0.885	0.733
Lewisburg	4.87	0.970	0.660
Manor	6.77	1.01	0.813
Mexico	1.90	4.33	0.648
Miami	4.64	2.27	0.700
Miamian	7.22	1.08	0.626
Nansene	3.58	2.04	0.607
Opequon	10.6	1.05	0.614
Palouse	4.35	0.925	0.735
Portneuf	4.30	2.08	0.702
Sharpsburg	4.46	0.529	0.665
Sverdrup	1.73	0.901	0.607
Tifton	2.20	0.746	0.638
Whitney	2.65	1.75	0.726
Williams	3.81	0.518	0.663
Woodward	3.61	1.18	0.606
Zahl	4.51	1.85	0.635

[a] Regression coefficients τ_c and K_r are used in the equation

$$\tau = \frac{1}{K_r}(D_c) + \tau_c$$

where shear stress and detachment capacity are in Pascals and kilograms per square meter per second, respectively.

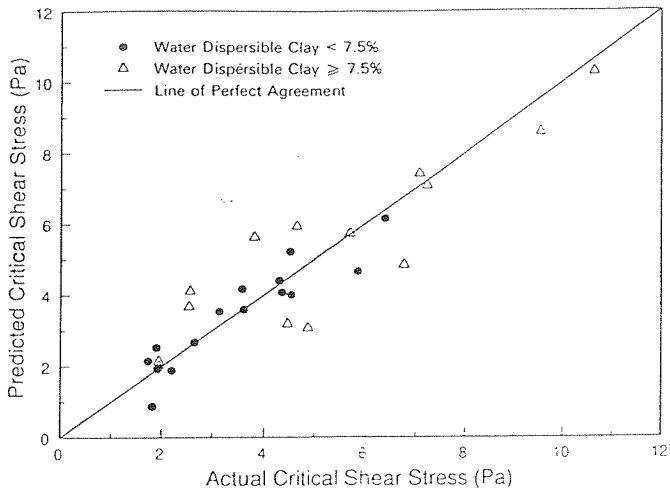

Fig. 4. Predicted vs. actual critical shear stress values.

Relating critical shear stress to soil properties

Step-wise multiple regression analyses were performed to relate critical shear stress values identified in Table 3 to soil properties presented in Table 2. Statistical analyses suggested that critical shear stress was significantly correlated to water dispersible clay. For soils with water dispersible clay content of less than 7.5%,

$$\tau_c = +0.216\ (\text{clay}) - 183\ (\text{coefficient of linear extensibility}) + 0.412\ (\text{soil water content at } 1.5\,\text{MPa}) + 0.780 \quad (6)$$

where clay and soil water content at 1.5 MPa are given as percentages, and coefficient of linear extensibility is in centimeters per centimeter. All the regression coefficients shown in eqn. (6) were significantly different from zero at the 95% confidence level. For soils with water dispersible clay content of 7.5% or greater,

$$\tau_c = 0.296\ (\text{calcium}) + 1.53\ (\text{iron}) + 7.75\ (\text{organic carbon}) - 11.4\ (\text{potassium}) - 0.535\ (\text{very fine sand}) - 0.208 \quad (7)$$

where calcium and potassium content are in centimoles per kilogram, and iron, organic carbon and very fine sand are given as percentages. All the regression coefficients shown in eqn. (7) were significantly different from zero at the 95% confidence level.

Values of τ_c were calculated for each of the experimental soils using soil survey data and eqns. (6) and (7). Results of the analyses are shown in Fig. 4. It can be seen from Fig. 4 that predicted and actual values of τ_c were similar.

Linear regression analyses were employed to compare predicted and actual values of τ_c. Results of the statistical analyses are shown in Table 4. Coefficient of determination values of 0.859 and 0.808 were found for eqns. (6) and (7), respectively.

The Students t-test was used to evaluate the hypotheses that the regression coefficients shown in Table 4 equal unity and the intercepts equal zero at the 95% confidence level. The slopes were not significantly different from unity, nor were the intercepts significantly different from zero. Thus, analyses of the experimental data suggests that eqns. (6) and (7) can be used to estimate τ_c.

RILL SOIL ERODIBILITY FACTOR

Determining the rill soil erodibility factor

Figure 3 shows shear stress versus sediment detachment capacity for a Barnes soil in North Dakota. The inverse of the slope of the regression line presented in Fig. 3 is defined as the rill soil erodibility factor. For the Barnes soil in North Dakota, the slope of the regression line was 189, which corresponds to a rill soil erodibility factor of $0.00529\,s\,m^{-1}$.

Linear regression analyses were used to determine rill soil erodibility factors for each of the other study locations. Results of the regression analyses are shown in Table 3. Rill soil erodibility factors were found to vary from $0.00276\,s\,m^{-1}$ for the Caribou soil to $0.0476\,s\,m^{-1}$ for the Amarillo soil.

Relating rill soil erodibility factors to soil properties

Rill soil erodibility factors identified in Table 3 were related to soil properties presented in Table 2 using step-wise multiple regression analyses. The rill soil erodibility factors were found to be significantly correlated to soil water content at 0.3 MPa. For sites with soil water content at 0.3 MPa of 23.0% or less,

$$K_r = -0.00294\ (\text{iron}) + 0.121\ (\text{sodium}) + 0.0113 \quad (8)$$

where iron content is given as a percentage and sodium concentration is in centimoles per kilogram. The regression coefficients shown in eqn. (8) were significantly different from zero at the 99% confidence level.

For sites with a soil water content at 0.3 MPa greater than 23.0%

$$K_r = 0.00436\ (\text{iron}) - 0.00412\ (\text{organic carbon}) - 0.000294\ (\text{sand}) + 0.00121\ (\text{very fine sand}) + 0.00551 \quad (9)$$

where iron, organic carbon, sand and very fine sand are given as percentages.

TABLE 4

Statistical analyses of predicted versus actual critical shear stress values

Regression equation	Coefficient of determination, r^2	F	β_1		β_0	
			Students t	Standard error	Students t	Standard error
Water dispersible clay < 7.5% Predicted = 0.890 actual + 0.341	0.859	79	−1.10	0.100	0.901	0.379
Water dispersible clay ⩾ 7.5% Predicted = 0.809 actual + 1.01	0.808	51	−1.68	0.114	1.51	0.669

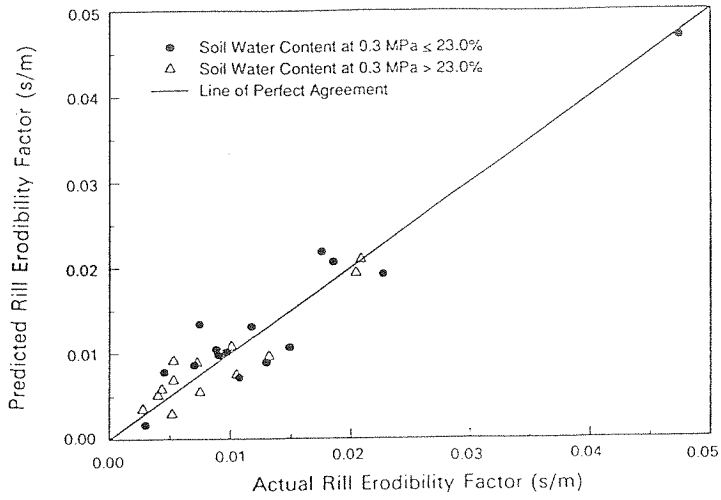

Fig. 5. Predicted vs. actual rill erodibility factors.

The regression coefficients shown in eqn. (9) were significantly different from zero at the 95% confidence level.

Soil survey data and eqns. (8) and (9) were used to calculate values of K_r for each of the experimental soils. Results of the analyses are presented in Fig. 5. Predicted and actual values of K_r shown in Fig. 5 can be seen to be similar.

Linear regression analyses were used to compare predicted and actual values of K_r. Results of the statistical analyses are presented in Table 5. Equations (8) and (9) produced coefficient of determination values of 0.915 and 0.865, respectively.

The hypotheses that the regression coefficients shown in Table 5 equal unity and the intercepts equal zero were evaluated at the 95% confidence level using the students *t*-test. The slopes were not significantly different from unity nor were the intercepts significantly different from zero. Thus, analyses of the experimental data suggests that eqns. (8) and (9) can be used to estimate rill soil erodibility factors.

CRITICAL FLOW RATES

Identifying critical flow rates

Flow rate versus slope-adjusted detachment capacity for the Barnes soil in North Dakota is shown in Fig. 6. Results obtained for this soil are also representative of the other experimental locations. It can be seen from Fig. 6 that the relationship between flow rate and slope-adjusted detachment

TABLE 5

Statistical analyses of predicted vs. actual regression coefficient K_r

Regression equation	Coefficient of determination, r^2	F	β_1		β_0	
			Students t	Standard error	Students t	Standard error
Soil water content at 0.3 MPa ⩽ 23.0%						
Predicted = 0.938 actual + 1.14	0.915	140	−0.789	0.079	0.837	1.37
Soil water content at 0.3 MPa > 23.0%						
Predicted = 0.866 actual + 1.21	0.865	77	−1.37	0.096	1.17	1.04

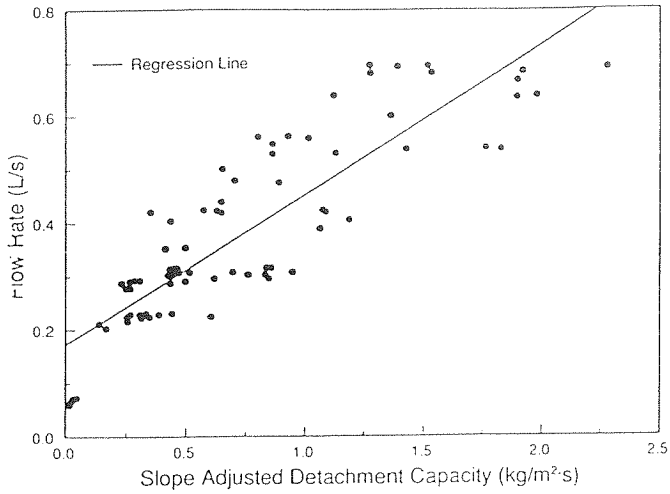

Fig. 6. Flow rate vs. slope adjusted sediment detachment capacity for a Barnes soil in North Dakota.

capacity can be well represented by a linear equation. Critical flow rate for initiation of rilling for the Barnes soil in North Dakota was $0.173\,l\,s^{-1}$.

Linear regression analyses were used to identify the critical flow rate values shown in Table 6. Flow rates required to initiate rilling varied widely between study locations. Critical flow rates ranged from $0.00247\,l\,s^{-1}$ for the Miami soil to $0.217\,l\,s^{-1}$ for the Pierre soil.

Relating critical flow rates to soil properties

Critical flow rate values identified in Table 6 were related to soil properties presented in Table 2 using step-wise multiple regression analyses. Statistical analyses suggested that critical flow rates were significantly correlated to silt content. For sites with silt content of 37.0% or less,

$$Q_c = 0.222\,(\text{aluminum}) + 0.0171\,(\text{cation exchange capacity}) - 0.0223\,(\text{magnesium}) - 0.00984\,(\text{soil water content at } 0.3\,\text{MPa}) + 0.00204\,(\text{very fine sand}) + 0.108 \quad (10)$$

where aluminum concentration, soil water content at 0.3 MPa and very fine sand are given as a percentage, and cation exchange capacity and magnesium content are in centimoles per kilogram. The regression coefficients shown in eqn. (10) were significantly different from zero at the 90% confidence level.

For sites with silt content greater than 37.0%

$$Q_c = 0.00373\,(\text{calcium}) + 0.0189\,(\text{magnesium}) + 0.0966\,(\text{organic carbon}) - 0.0537\,(\text{potassium}) + 0.00462\,(\text{soil water content at } 0.3\,\text{MPa}) - 0.130 \quad (11)$$

TABLE 6

Statistical analyses of equations used to relate rill flow rate to detachment capacity

Soil	Q_c[a] ($l\,s^{-1}$)	K_f[a] ($kg\,l^{-1}\,m^{-2}$)	Coefficient of determination, r^2
Academy	0.177	9.23	0.658
Amarillo	0.164	29.3	0.613
Barnes-MN	0.152	6.67	0.704
Barnes-ND	0.173	3.57	0.754
Caribou	0.198	1.22	0.624
Cecil	0.0767	3.28	0.693
Collamer	0.0747	7.07	0.809
Frederick	0.0912	1.63	0.709
Grenada	0.143	4.96	0.657
Heiden	0.0947	8.36	0.614
Hersh	1.500	9.72	0.638
Hiwassee	0.00432	6.11	0.731
Lewisburg	0.110	4.55	0.752
Manor	0.122	4.76	0.855
Mexico	0.132	2.31	0.678
Miami	0.00247	6.42	0.730
Miamian	0.0955	4.80	0.601
Nansene	0.106	16.2	0.615
Opequon	0.147	2.45	0.639
Palouse	0.115	6.00	0.731
Pierre	0.217	13.8	0.609
Portneuf	0.140	13.3	0.669
Sharpsburg	0.153	3.53	0.734
Sverdrup	0.166	10.5	0.612
Tifton	0.125	4.58	0.703
Whitney	0.0880	9.90	0.647
Williams	0.203	3.70	0.629
Woodward	0.0602	7.61	0.653
Zahl	0.184	12.3	0.640

[a] Regression coefficients Q_c and K_f are used in the equation

$$Q = \frac{1}{K_f}\left(\frac{D_c}{S^{3/2}}\right) + Q_c$$

where flow rate and detachment capacity are in liters per second and kilograms per square meter per second, respectively, and slope is given as a fraction.

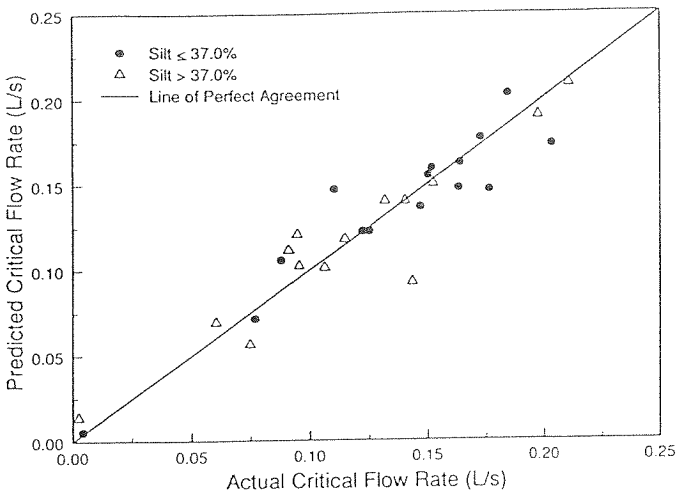

Fig. 7. Predicted vs. actual critical flow rates.

where calcium, magnesium, and potassium are in centimoles per kilogram, and organic carbon and soil water content at 0.3 MPa are given as a percentage. All the regression coefficients shown in eqn. (11) were significantly different from zero at the 90% confidence level.

Values of Q_c were calculated for each of the experimental soils using soil survey data and eqns. (10) and (11). Results of the analyses are shown in Fig. 7. Predicted and actual values of Q_c shown in Fig. 7 can be seen to be similar.

Linear regression analyses were used to compare predicted and actual values of Q_c. Results of the statistical analyses are shown in Table 7. Coefficient of determination values of 0.878 and 0.882 were found for eqns. (10) and (11), respectively.

The Students t-test was used to evaluate the hypotheses that the regression coefficients shown in Table 7 equal unity and the intercepts equal zero at the 95% confidence level. The slopes were not significantly different from unity nor were the intercepts significantly different from zero. Thus, analyses of the experimental data suggests that eqns. (10) and (11) can be used to estimate Q_c.

FLOW-RELATED RILL SOIL ERODIBILITY FACTORS

Identifying flow-related rill soil erodibility factors

Figure 6 shows flow rate versus slope-adjusted detachment capacity for the Barnes soil in North Dakota. The flow-related rill soil erodibility factor is represented by the inverse of the slope of the regression line presented in Fig. 6. For the Barnes soil in North Dakota, the slope of the regression line was

TABLE 7

Statistical analyses of predicted vs. actual critical flow rate values

Regression equation	Coefficient of determination, r^2	F	β_1		β_0	
			Students t	Standard error	Students t	Standard error
Silt $\leqslant$ *37.0%* Predicted = 0.880 actual + 0.016	0.878	93	−1.32	0.091	1.22	0.013
Silt > *37.0%* Predicted = 0.883 actual + 0.013	0.882	90	−1.26	0.093	1.14	0.012

0.280, which corresponds to a flow-related rill soil erodibility factor of $3.57\,kg\,l^{-1}\,m^{-2}$.

Flow-related rill soil erodibility factors were determined for each of the other study locations using linear regression analyses. Results of the regression analyses are shown in Table 6. Flow-related rill soil erodibility factors were found to vary from $1.22\,kg\,l^{-1}\,m^{-2}$ for the Caribou soil to $29.3\,kg\,l^{-1}\,m^{-2}$ for the Amarillo soil.

Relating flow-related rill soil erodibility factors to soil properties

Step-wise multiple regression analysis was used to relate the flow-related rill soil erodibility factors identified in Table 6 to soil properties presented in Table 2. The flow-related rill soil erodibility factors were found to be significantly correlated to sand content. For sites with sand content of 40.0% or less,

$$K_f = -245\ (\text{coefficient of linear extensibility}) + 0.971\ (\text{clay}) + 0.336\ (\text{silt}) + 0.275\ (\text{soil water content at 0.3 MPa}) + 1.04\ (\text{very fine sand}) - 43.9 \quad (12)$$

where coefficient of linear extensibility is in centimeters per centimeter and clay, silt, soil water content at 0.3 MPa, and very fine sand are given as a percentage. All the regression coefficients shown in eqn. (12) were significantly different from zero at the 90% confidence level.

For sites with sand content greater than 40.0%,

$$K_f = 329\ (\text{coefficient of linear extensibility}) + 76.3\ (\text{sodium}) - 20.3\ (\text{potassium}) - 0.743\ (\text{water dispersible clay}) + 11.7 \quad (13)$$

where coefficient of linear extensibility is in centimeters per centimeter, sodium and potassium are in centimoles per kilogram, and water dispersible clay is given as a percentage. All the regression coefficients shown in eqn. (13) were significantly different from zero at the 90% confidence level.

Values of K_f were calculated for each of the experimental soils using soil survey data and eqns. (12) and (13). Results of the analyses are shown in Fig. 8. Predicted and actual values of K_f shown in Fig. 8 can be seen to be similar.

Linear regression analyses were used to compare predicted and actual values of K_f. Results of the statistical analyses are presented in Table 8. Equations (12) and (13) produced coefficient of determination values of 0.906 and 0.837, respectively.

The Students *t*-test was used to evaluate the hypotheses that the regression coefficients shown in Table 8 equal unity and the intercepts equal zero at the 95% confidence level. The slopes were not significantly different from unity

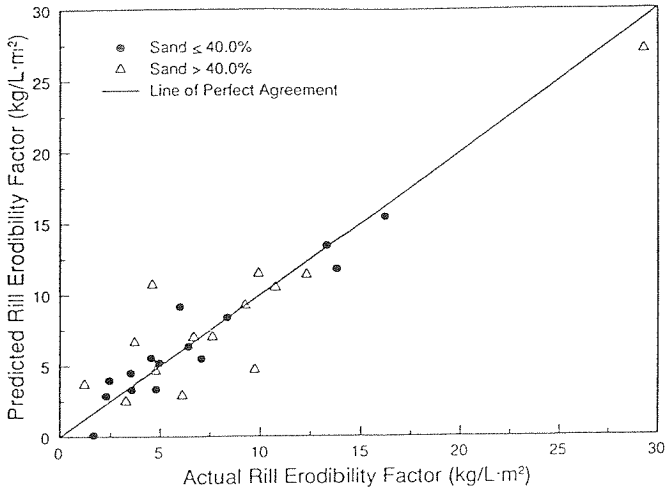

Fig. 8. Predicted vs. actual flow related rill erodibility factors.

nor were the intercepts significantly different from zero. Thus, analyses of the experimental data suggests that eqns. (12) and (13) can be used to estimate flow-related rill soil erodibility factors.

LIMITATIONS OF THE REGRESSION EQUATIONS

Although reasonable estimates of critical shear stress and critical flow rates were provided by the regression equations, other factors may limit their application in field situations. For example, crop residues and rock fragments were absent from the sites where the experimental data used to parameterize the regression equations were obtained. Crop residue cover could serve to protect rill and interrill areas from soil detachment. Soil detachment may also decrease as channel armoring develops, if soils contain rock fragments. Critical shear stress and critical flow rates for sites where crop residue or rock fragments are present may be substantially larger than estimates obtained using equations presented in this study.

Temporal variations in critical shear stress and critical flow rates may also occur. These differences have been attributed to changes in soil cohesion, rainfall-induced soil consolidation, and development of root fabric. Critical shear stress and critical flow rates identified in this study are strictly applicable only for conditions immediately following tillage. At present, procedures for estimating temporal effects on critical shear stress and critical flow rates have not been identified.

Values of K_r and K_f were determined for bare unconsolidated soil conditions existing immediately after tillage. Soil erodibility may be affected

TABLE 8

Statistical analyses of predicted vs. actual flow related rill soil erodibility factors

Regression equation	Coefficient of determination, r^2	F	β_1		β_0	
			Students t	Standard error	Students t	Standard error
Sand $\leqslant$ *40.0%* Predicted = 0.906 actual + 0.625	0.906	125	− 1.16	0.081	0.976	0.640
Sand > *40.0%* Predicted = 0.838 actual + 1.41	0.837	62	− 1.52	0.107	1.23	1.14

by soil consolidation, below-ground residue, and freeze–thaw conditions. Methods for calculating the effects of soil consolidation on erodibility were identified by Nearing et al. (1988). Brown et al. (1989) developed relationships for adjusting rill erodibility for below-ground residue.

This study was conducted on cropland soils where surface residue had been removed and the areas were maintained free of vegetation for several months. The sites were tilled immediately before testing and were, therefore, in a highly erosive condition. The regression equations developed in this study should not be applied to pasture or rangeland areas with much different soil and vegetative characteristics.

SUMMARY AND CONCLUSIONS

Hydraulic conditions required to initiate rilling were identified in this study. Linear equations were used to relate shear stress values and flow rates to rill sediment detachment capacity. The intercept of the linear equations provided estimates of critical shear stress and critical flow rate.

Runoff and erosion data collected on soils located throughout the USA were used to determine critical shear stress values and critical flow rates. The experimental sites were selected to cover a broad range of soil properties. On each of the sites, crop residue had been removed, moldboard plowing and disking had occurred, and preformed rills had been constructed.

Selected soil properties were measured at each of the experimental locations. Critical shear stress values and critical flow rates were related to site-specific soil properties using multiple regression analysis. Close agreement was found between predicted and actual values.

Process-based models for predicting runoff and erosion on upland areas require information on flow hydraulics and soil erodibility. Procedures for estimating hydraulic conditions required to create rills were identified in this investigation. This information will improve our ability to understand and properly model upland runoff and erosion processes.

ACKNOWLEDGMENTS

This paper is a contribution from USDA-ARS, in cooperation with the Agricultural Research Division, University of Nebraska, Lincoln, and is published as Journal Series No. 9647.

REFERENCES

Brown, L.C., Foster, G.R. and Beasley, D.B., 1989. Rill erosion as affected by incorporated crop residue and seasonal consolidation. Trans. ASAE, 32(6): 1967–1978.

Elliot, W.J., Liebenow, A.M., Laflen, J.M. and Kohl, K.D., 1989. A compendium of soil erodibility data from WEPP cropland soil field erodibility experiments 1987 and 88. NSERL Rep. No. 3, USDA-ARS, West Lafayette, IN, 317 pp.

Foster, G.R., 1982. Modeling the erosion process. In: C.T. Haan, H.P. Johnson and D.L. Brakensiek (Editors), Hydrologic Modeling of Small Watersheds. American Society of Agricultural Engineers, St. Joseph, MI, pp. 297–380.

Laursen, E.M., 1958. The total sediment load of streams. J. Hydraul. Div., ASCE 123(1): 195–206.

Nearing, M.A., West, L.T. and Brown, L.C., 1988. A consolidation model for estimating changes in rill erodibility. Trans. ASAE, 31(3): 696–700.

Nearing, M.A., Foster, G.R., Lane, L.J. and Finkner, S.C., 1989. A process-based soil erosion model for USDA-Water Erosion Prediction Project technology. Trans. ASAE, 32(5): 1587–1593.

Schoklitsch, A., 1957. River bed degradation below large capacity reservoir. Trans. ASCE, 122: 688–695.

Soil Survey Staff, 1984. Procedures for collecting soil samples and methods of analysis for soil survey. USDA-SCS Soil Survey Investigations Rep. No. 1., U.S. Government Printing Office, Washington, DC.

Swanson, N.P., 1965. Rotating-boom rainfall simulator. Trans. ASAE, 8(1): 71–72.